Theor Chim Acta (1994) 88: 217–232

Theoretica Chimica Acta

Ab initio investigations of the bound rovibrational levels of NeH_2^+, $NeHD^+$, and NeD_2^+*

Ralph Jaquet
Theoretische Chemie, Universität Siegen, D-57068 Siegen, Germany

Received April 1, 1993/Accepted September 3, 1993

Summary. Bound rovibrational levels have been calculated for NeH_2^+, $NeHD^+$, and NeD_2^+ using three recent fits to an accurate *ab initio* PES. The NeH_2^+ molecule behaves essentially as a linear molecule, the predicted rotational constant is 2.57 cm^{-1}. The fundamental frequencies are 811, 1189, and 1748 cm^{-1} for the Ne–H_2^+ stretch, the Ne–H_2^+ bend and H_2^+ stretching modes, respectively.

Key words: NeH_2^+ – $NeHD^+$ – NeD_2^+ – Bound vibrational levels

1 Introduction

There has been great interest over the last two decades on the chemistry and physics of molecular cluster ions containing rare gases (He, Ne, etc.) and molecular hydrogen [1]. For the system NeH_2^+ both cell and beam experiments have been performed to study the reaction [2]:

$$Ne + H_2^+ \rightarrow NeH^+ + H \qquad (\Delta H_0^0 = 0.57\ eV). \tag{1}$$

In particular, the influence of vibrational excitation of H_2^+ on the reaction probability has been analyzed. On the theoretical side, there have been several previous attempts to generate an accurate potential energy surface (PES) for Eq. (1) [3–6] and several scattering calculations both at the level of quasiclassical trajectories [7–10] and with quantum scattering methods with and without geometrical limitations [9, 11].

The rovibrational spectrum of NeH_2^+, i.e. its bound vibrational levels, has not been studied, neither theoretically nor experimentally. From quantum chemical *ab initio* calculations [9] it is known that NeH_2^+ has a collinear equilibrium geometry with a well depth of only 0.52 eV = 4194 cm^{-1}. The whole ground-state potential surface is rather shallow and extends over a wide range since it is dominated by electrostatic and induction forces which decay only with R^{-4}. There is a barrier of ca. 0.37 eV = 2984 cm^{-1} for the internal rotation – i.e. from the collinear over the perpendicular to the equivalent collinear form – which leads to the expectation that

* Dedicated to the 60th birthday of Prof. W. Kutzelnigg, Bochum

the molecules, once formed in a reaction, should be relatively stable in collinear geometry and should have several rotational and vibrational bound states.

Two years ago we had calculated a new 3D-PES by means of the coupled electron pair approach (CEPA) [10]. This PES was used for quasiclassical trajectory calculations for Eq. (1); the calculated reaction probabilities agreed very satisfactorily with the experimental data [2e, 2g]. However, in order to perform very accurate calculations for the rovibrational bound states and for quantum mechanical reaction probabilities it turned out to be necessary to improve this 3D-PES (by generating more points). In particular in the asymptotic region more points were needed in order to obtain the correct asymptotic dissociation behaviour. For the analytic representation of the surface better functional forms were used. Three different fits to the *ab initio* points were determined whose specific qualities have been discussed in [12].

As previous quantum scattering calculations have shown [9, 11] resonance structures in the cross sections are very pronounced at low energies, originating from the underlying bound states in the interaction region. The object of the current work is therefore to calculate the bound rovibrational energy levels of the NeH_2^+, $NeHD^+$, and NeD_2^+ ions. Comparable calculations have been performed for HeH_2^+ and its isotopomers by Tennyson and Miller [13].

2 Potential energy surface and calculation of rovibrational energy levels

The three different potential energy surfaces (PES) that we will be using in the present work were obtained from a three-dimensional fit of the $^2A'$ ground state energy points of Eq. (1) where a number of functional forms available for surface fitting were investigated. Results are described in [12]. 225 *ab initio* points (calculated with the open-shell CEPA approach [14]) were used to cover the decisive part of the surface, i.e. the inner repulsive walls, the entrance and exit channels with the correct asymptotic forms, saddle points of the reaction surface and the potential minimum area. Compared to earlier calculations, using an extended LEPS-Conroy fit [10], the well depth is lowered by 0.03 eV, Ishtwan et al. [19] report a value of $E_{\min,\,180°} = -0.53\,\text{eV} = -4275\,\text{cm}^{-1}$, DIM [3, 6] and SCF [5, 6] surfaces are about half as deep as these new surfaces.

Fit 1 uses a functional form suggested by Joseph and Sathyamurthy [15] which was first introduced by Sorbie and Murrell [16]. Fit 2 is a functional form used by Schinke [17] and the third fit is a functional form used by Aguado and Paniagua [18]. All the functions consist of two-body and one three-body terms. In the case of Fit 3 a maximum of 55 linear coefficients had to be determined. Contour plots for the three different surfaces (in jacobi coordinates) are given in Fig. 1. Further plots can be found in [10, 12].

All three surfaces have root mean-square-errors (i.e. standard deviations) of less than 0.03 eV = 242 cm^{-1}. The errors are even smaller than 0.022 eV for Fit 1 and smaller than 0.013 eV for Fit 3 for angles ($\measuredangle$(Ne–H–H)) between 180° and 90° where the deepest potential energy minimum is situated (with respect to the jacobi coordinate θ, see Fig. 1a, the potential has a double minimum shape). For further information see [12].

Some characteristics of the three surfaces are summarized in Table 1. Fit 3 is probably the most appropriate form to use in dynamic scattering calculations, because it does not have spurious minima even in those areas accessible only at

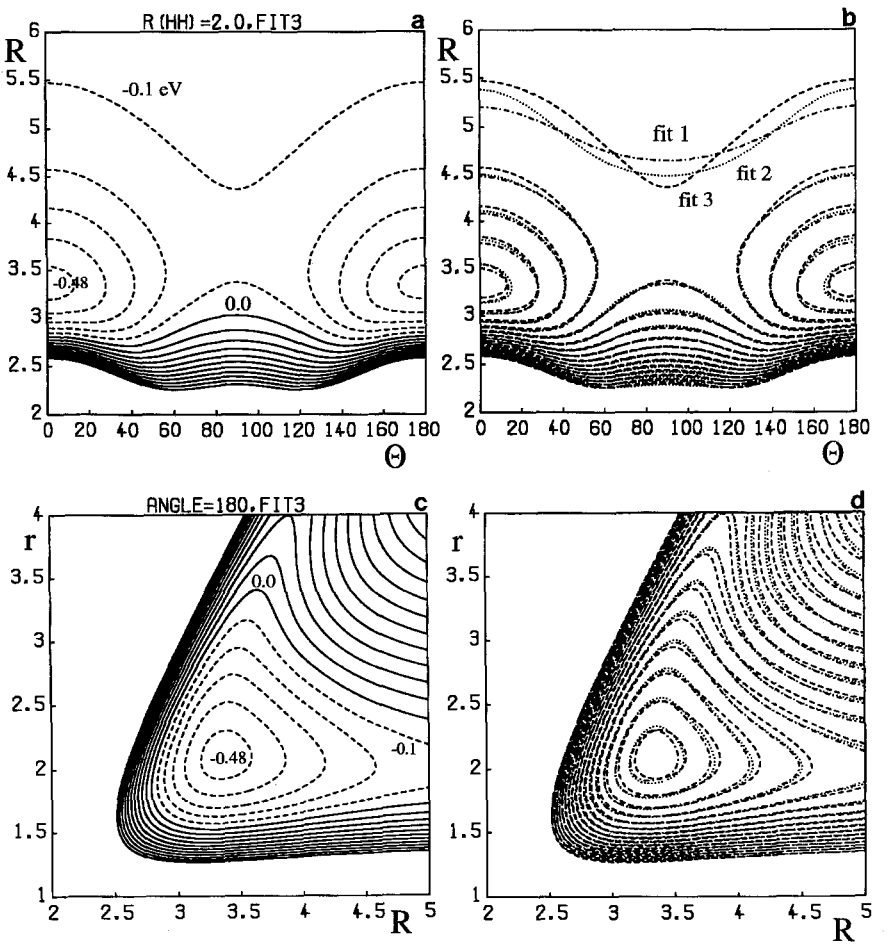

Fig. 1a–d. [NeH_2^+]: Contour plot of the potential energy surface in jacobi coordinates. **a)** Plot for Fit 3 with $r(H_2) = 2.0\ a_0$ fixed. **b)** Comparison of the 3 fits for the coordinates R and θ. **c)** Plot for Fit 3 with $\theta = 180°$ fixed. **d)** Comparison of the 3 fits for the coordinates r and R. R is the distance between Ne and the center of mass of H_2^+, θ is the angle between R and the diatomic bond r of H_2^+. Contours are given in steps of 0.1 eV

higher scattering energies. Bound-state calculations on these three surfaces can be another test to show how different the three surfaces are.

The variational calculations for the rovibrational states are performed using the variational method developed by Sutcliffe and Tennyson [20] for treating triatomic molecules and implemented in the program package TRIATOM of Tennyson and Miller [21]. These authors performed similar calculations for comparable molecules like HeH_2^+ [13], H_3^+ [22], etc. A comparison with finite element calculations using the hyperspherical coordinate method will be presented in a later paper [23].

The calculations are performed using scattering coordinates $R(\text{Ne–}H_2^+)$, $r(H_2^+)$, and $\theta(R, r)$. The basis functions are written as products of one-dimensional Morse

Table 1. Comparison of geometries and energies for the minima on the NeH_2^+, $^2A'$ surface at different angles. Energies are in cm^{-1} and distances in bohr

Angle θ'[c]	R_{NeH}	R_{HH}	E_{min}[a]	Source
180°	2.27	2.08	− 4140	Fit 1
	2.28	2.08	− 4218	Fit 2
	2.31	2.10	− 4134	Fit 3
	2.31	2.08	− 3871	[10]
	2.26	2.07	− 4274	[19]
120°	2.68	1.99	− 2191	Fit 1
	2.70	1.99	− 2156	Fit 2
	2.69	2.03	− 2200	Fit 3
	2.53	2.00	− 2016	[10]
90°	3.54	1.94	− 1252	Fit 1
	3.56	1.95	− 1259	Fit 2
	3.44	1.96	− 1084	Fit 3
	3.49	2.00	− 1048	[10]
Angle θ[c]	$R_{Ne-H_2^+}$	R_{HH}	E_{min}[a, b]	Source
90°	3.75	1.94	− 1175	Fit 1
	3.75	1.95	− 1190	Fit 2
	3.67	1.96	− 957	Fit 3

[a] Relative to $Ne + H_2^+$

[b] Barrier for internal rotation of H_2^+

[c] $\theta' = \sphericalangle(Ne\text{–}H\text{–}H^+)$, $\theta = \sphericalangle(R(Ne\text{–}H_2^+), r(H_2^+))$

oscillator functions for the R and r coordinates and associated Legendre functions $\Theta_{j,k}(\theta)$ (j represents the rotation of the H_2^+ and k is the projection of the total angular momentum J on the molecular axis). Because the equilibrium structure is linear, k is nearly a good quantum number. First Morse parameters for the Morse functions were used which result from a separate fit to the H_2^+ and $Ne\text{–}H_2^+$ ($r = 2.1$) potential energy curves. However, optimal Morse functions for the triatomic bound state calculations are not equivalent to those optimal for the asymptotic H_2^+-potential or the collinear $Ne\text{–}H_2^+$ (with rigid H_2^+) potential. So the following parameters have been chosen: $R_e = 3.47\ a_0$, $D_R = 0.015$ au, $\omega_R = 0.0025$ au and $r_e = 2.20\ a_0$, $D_r = 0.05$ au, $\omega_r = 0.009$ au. These parameters are similar to those used for HeH_2^+ [13]. For HD^+ $\omega_r = 0.0075$ au and for D_2^+ $\omega_r = 0.006$ au was used. The following atomic masses for Ne, H, D have been taken: $m_{Ne} = 20.164901$ au, $m_H = 1.007825$ au, $m_D = 2.016490$ au.

Because the potential surface extends over a rather large area and in order to implement sufficient flexibility up to 13 radial functions in R and r and 28 angular functions have been used. Symmetry has been used for *para*-H_2^+ (j even) and *ortho*-H_2^+ (j odd). For testing purposes the lowest 600 and 1200 product functions have been used, which show that with 600 product functions the results for the lowest 10 bound states (of the same symmetry) are accurate within 1 cm^{-1} (most of the results are more accurate than 0.1 cm^{-1}). The uncertainties attributable to the different fitting procedures and the differences between the three fitted surfaces are much larger.

$J = 0, 1, 2$ calculations (parity e and f) have been performed where the 200 lowest solutions of the vibrational problem for each k were used to get convergence for the fully Coriolis coupling ($J = 1.2$) calculations. The accuracy for the rotational excited states using 600 or 1200 product functions is the same as for the $J = 0$ states. States with parity $(-1)^{J+p}$ are labelled $e(p = 0)$ or $f(p = 1)$ [24]. Only states with even quanta of the bending mode exist for $J = 0$.

3 Results and discussion

Tables 2–4 show the results of our calculations for $J = 0$ for NeH_2^+, $NeHD^+$, and NeD_2^+ for the three different surfaces. For better understanding, contour plots of the wavefunctions are given in the scattering coordinates R and angle θ. Table 5 presents and compares the results for even and odd states of NeH_2^+ and NeD_2^+ ($J = 0$). Table 6 presents results for NeH_2^+ for total angular momentum $J = 1, 2$ compared to $J = 0$ and Table 7 summarizes the results for the lowest $J = 1$ rovibrational levels of the isotopomers of NeH_2^+.

The absolute binding energies in Tables 2–7 are given relative to the dissociation products of atomic Ne and the corresponding H_2^+ isotopes. The assignments of the above defined (see Table 2) quantum numbers is only approximate (especially for some higher states) and can be derived from the Figs. 2–5. With respect to the θ coordinate the potential has a double minimum form and the wavefunctions are classified as symmetric (j even, *para*-H_2^+) or antisymmetric (j odd, *ortho*-H_2^+). The

Table 2. Comparison of the calculated rovibrational levels (in cm^{-1}) for NeH_2^+, $J = 0$, $j = even$ using three different surfaces (Fit 1, 2, 3). The frequencies are given relative to the vibrational ground state energy, which in turn is given relative to the $Ne + H_2^+$ dissociation limit. The vibrational states are labelled with the quantum numbers v according to the degree of excitation: $v_r = H_2^+$ stretching mode, $v_b = Ne{-}H_2^+$ bending mode and $v_s = Ne{-}H_2^+$ stretching mode

		Fit		1	2	3
#[a]		E_{000}		−2070.23	−2112.91	−2108.45
	v_r	v_b	v_s			
2	0	0	0	0.0	0.0	0.0
3	0	0	1	849.5	858.6	810.7
5	0	2	0	1198.0	1228.4	1189.4
7	0	0	2	1566.6	1587.3	1513.6
10	1	0	0[b]	1726.6	1740.3	1747.6
11	0	2	1	1884.7	1919.4	1863.6
13	0	4	1	2104.8	2146.5	2108.1
15	0	0	3	2171.8	2203.8	2139.5
17	0	2	2	2366.8	2422.1	2394.1
19				2456.6	2492.6	2534.5
				2578.1	2610.8	2582.8
				2698.8	2744.3	2700.8
				2744.7	2795.0	2776.2

[a] Number of plot in Fig. 2

[b] With a strong admixture of (0, 0, 1)

Table 3. Same as Table 2, but for $NeDH^+$ and $NeHD^+$

v_r	v_b	v_s	#[a]	$NeDH^+$	#[a]	$NeHD^+$
				Fit 1		
0	0	0	1	− 2413.62	2	− 2283.50
0	0	1	3	743.8	4	689.1
0	2	0	5	991.2	6	1137.6
0	0	2	7	1386.5	8	1341.1
1	0	1	9	1479.5	11	1540.2[b]
1	2	1	10	1625.1	12	1738.2[c]
				Fit 2		
0	0	0		− 2461.62		− 2329.45
0	0	1		748.5		697.8
0	2	0		1021.8		1164.7
0	0	2		1400.1		1358.7
1	0	1		1493.9		1550.1[b]
1	2	1		1659.1		1766.7[c]
				Fit 3		
0	0	0		− 2441.44		− 2324.09
0	0	1		699.2		664.8
0	2	0		977.1		1122.7
0	0	2		1321.4		1300.2
1	0	1		1515.3		1554.2[b]
1	2	1		1585.7		1713.8[c]

[a] Number of plot in Fig. 3
[b] (1, 2, 1), see Fig. 3
[c] (0, 2, 2), see Fig. 3

Table 4. Same as Table 2, but for NeD_2^+

		Fit		1	2	3
#[a]		E_{000}		− 2645.21	− 2697.01	− 2673.79
	v_r	v_b	v_s			
1	0	0	0	0.0	0.0	0.0
4	0	0	1	656.9	662.9	622.5
5	0	2	0	902.8	930.1	888.7
8	1	0	0[b]	1210.4	1221.4	1180.8
10	1	0	2[b]	1282.6	1294.5	1271.4
11	0	2	1	1486.7	1516.7	1446.7
13	0	4	0	1682.3	1728.0	1675.2
16	0	0	3	1758.5	1781.5	1696.0
18				1927.7	1950.1	1913.9
20				1994.5	2032.0	1950.1
				2159.8	2198.5	2159.0
				2191.3	2229.2	2176.5

[a] Number of plot in Fig. 4
[b] Strong coupling of the R and r mode, see Fig. 5

Table 5. Zero-point energies and vibrational band origins of the symmetric isotopomers of NeH_2^+. Energies in cm^{-1}. Explanations see Table 2

			j even				*j* odd			
v_r	v_b	v_s	#[a]	NeH_2^+	#[b]	NeD_2^+	#[a]	NeH_2^+	#[b]	NeD_2^+
						Fit 1				
0	0	0	2	− 2070.23	1	− 2645.21	1	− 2070.24	2	− 2645.21
0	0	1	3	849.5	4	656.9	4	849.4	3	656.9
0	2	0	5	1198.0	5	902.8	6	1198.1	6	902.8
0(1)	0	2	7	1566.6	10	1282.6[c]	8	1566.6	9	1282.5[c]
1	0	0	10	1726.6	8	1210.6[c]	9	1726.0	7	1210.4[c]
0	2	1	11	1884.7	11	1486.7	12	1888.5	12	1486.7
0	4	1(0)	13	2104.8	13	1682.3	14	2135.7	14	1682.3
						Fit 2				
0	0	0		− 2112.91		− 2697.01		− 2112.91		− 2697.01
0	0	1		858.6		662.9		858.6		662.9
0	2	0		1228.4		930.1		1228.5		930.1
0(1)	0	2		1587.3		1294.5[c]		1587.3		1294.5[c]
1	0	0		1740.3		1221.4[c]		1739.8		1221.4[c]
0	2	1		1919.4		1516.7		1922.8		1516.7
0	4	1(0)		2146.5		1728.0		2175.1		1728.1
						Fit 3				
0	0	0		− 2108.45		− 2673.80		− 2108.45		− 2673.80
0	0	1		810.7		622.5		810.7		622.5
0	2	0		1189.4		888.7		1189.5		888.7
0(1)	0	2		1513.6		1271.4[c]		1513.6		1271.4[c]
1	0	0		1747.6		1180.6[c]		1747.2		1180.6[c]
0	2	1		1863.6		1446.7		1864.5		1446.7
0	4	1(0)		2108.1		1675.2		2108.0		1675.2

[a] Number of plot in Fig. 2

[b] Number of plot in Fig. 4

[c] In NeD_2^+ an energetically different order with respect to the given quantum numbers than in NeH_2^+

quantum numbers with respect to the bending mode are classified 0, 2, 4, ... In Tables 2 and 4 only the values for the symmetric states are listed, because eigenvalues for *j* even and *j* odd states are very similar, at least for the lowest quantum numbers (see in addition the headlines in Figs. 2 and 4).

The results presented in Table 2 are calculated for 600 product basis functions. For the lowest 10 states a similar accuracy is obtained if the basis is extended to 1200 product functions ($< 1\ cm^{-1}$), while for the next higher 10 states a few of them change by up to $10\ cm^{-1}$. The zero point energy (ZPE) ($= E_{000}$ in the Tables 2–4) amounts to about one half of the electronic binding energy of $4140\ cm^{-1}$ (Fit 1), such that the well depth is reduced by nearly one half after inclusion of the ZPE.

Table 6a. Fit 1: Calculated rovibrational levels (in cm^{-1}) for NeH_2^+. The frequencies of the $J = 0$ levels are given relative to the ground state, which in turn is given relative to the $Ne + H_2^+$ dissociation limit. The rotationally excited levels are given relative to the corresponding $J = 0$ vibrational levels

(i) Only the complexes dissociating to *para*-H_2^+ (*j even*) are considered

v_r	v_b	v_s	$J = 0$	$J = 1^e$		$J = 1^f$	$J = 2^e$			$J = 2^f$	
				$k = 0$	$k = 1$	$k = 1$	$k = 0$	$k = 1$	$k = 2$	$k = 1$	$k = 2$
0	0	0	(−2070.23)	5.25	650.35	650.44	15.73	660.86	1298.23	661.12	1298.23
0	0	1	849.46	4.98	583.42	583.54	14.94	593.22	1141.84	593.58	1141.84
0	2	0	1198.02	5.22	528.58	528.83	15.66	538.65	1022.08	539.40	1022.09
0	0	2	1566.66	4.69	510.32	510.53	14.07	519.13		519.74	
1	0	0	1726.64	5.08	576.88	579.22	15.25				
0	2	1	1884.74	4.85	645.97	650.93	14.54				
0	4	1	2104.88	5.53	469.49	470.73	16.57				
0	0	3	2271.57	4.41	437.82	437.73	13.23				

(ii) Only the complexes dissociating to *ortho*-H_2^+ (*j odd*) are considered

v_r	v_b	v_s	$J = 0$	$J = 1^e$		$J = 1^f$	$J = 2^e$			$J = 2^f$	
				$k = 0$	$k = 1$	$k = 1$	$k = 0$	$k = 1$	$k = 2$	$k = 1$	$k = 2$
0	0	0	(−2070.23)	5.24	650.34	650.43	15.73	660.85	1298.29	661.10	1298.29
0	0	1	849.45	4.98	583.38	583.49	14.94	593.18	1144.34	593.53	1144.33
0	2	0	1198.13	5.21	526.04	526.18	15.64	536.41	1040.77	536.81	1039.06
0	0	2	1566.64	4.69	509.20	509.37	14.07	518.12		518.61	
1	0	0	1726.04	5.08	512.56	512.56	15.25				
0	2	1	1888.51	4.73	486.30	486.38	14.20				
0	4	1	2135.66	4.29	338.03	337.82	12.92				
0	0	3	2173.06	4.32	393.54	394.11	12.98				

Table 6b. Same as Table 6a, but from Fit 2

(i) Only the complexes dissociating to *para*-H_2^+ (*j even*) are considered

v_r	v_b	v_s	$J=0$	$J=1^e$		$J=1^f$	$J=2^e$			$J=2^f$	
				$k=0$	$k=1$	$k=1$	$k=0$	$k=1$	$k=2$	$k=1$	$k=2$
0	0	0	(−2112.91)	5.22	673.50	673.58	15.66	683.94	1338.97	684.20	1338.97
0	0	1	858.62	4.97	602.64	602.76	14.90	612.41	1175.27	612.78	1175.27
0	2	0	1228.41	5.20	540.31	540.55	15.59	550.35	1039.35	551.07	1039.35
0	0	2	1587.29	4.71	529.87	530.01	14.11	538.66		539.34	
1	0	0	1740.24	5.06	603.21	605.33	15.17				
0	2	1	1919.43	4.85	495.77	496.22	14.56				
0	4	1	2146.45	5.46	473.79	473.31	16.34				
0	0	3	2203.81	4.48	455.88	455.90	13.44				

(ii) Only the complexes dissociating to *ortho*-H_2^+ (*j odd*) are considered

v_r	v_b	v_s	$J=0$	$J=1^e$		$J=1^f$	$J=2^e$			$J=2^f$	
				$k=0$	$k=1$	$k=1$	$k=0$	$k=1$	$k=2$	$k=1$	$k=2$
0	0	0	(−2112.91)	5.22	673.48	673.57	15.65	683.93	1339.02	684.19	1339.02
0	0	1	858.62	4.97	602.59	602.71	14.90	612.37	1177.70	612.73	1177.70
0	2	0	1228.49	5.18	537.91	538.05	15.56	548.23	1074.84	548.63	1082.69
0	0	2	1587.29	4.71	529.04	529.23	14.11	537.93		538.48	
1	0	0	1739.80	5.06	539.85	538.55	15.17				
0	2	1	1922.82	4.75	490.81	490.91	14.24				
0	4	1	2175.10	4.25	337.37	337.22	12.79				
0	0	3	2208.42	4.30	418.31	418.02	12.91				

Table 6c. Same as Table 6a, but from Fit 3

(i) Only the complexes dissociating to *para*-H_2^+ (*j even*) are considered

v_r	v_b	v_s	$J=0$	$J=1^e$		$J=1^f$	$J=2^e$			$J=2^f$	
				$k=0$	$k=1$	$k=1$	$k=0$	$k=1$	$k=2$	$k=1$	$k=2$
0	0	0	(−2108.45)	5.14	637.00	637.08	15.42	647.29	1275.31	647.54	1275.31
0	0	1	810.72	4.89	577.20	577.32	14.66	586.86	1146.38	587.21	1146.38
0	2	0	1189.42	5.14	536.09	536.31	15.43	546.09	1047.32	546.74	1047.33
0	0	2	1513.65	4.59	513.31	513.50	13.78	522.13		522.70	
1	0	0	1747.59	5.06	570.69	571.41	15.19	578.56		580.70	
0	2	1	1863.65	4.77	526.50	526.75	14.30				
0	4	1	2108.12	4.37	445.53	444.90	13.10				
0	0	3	2139.45	5.39	464.47	462.71	16.16				

(ii) Only the complexes dissociating to *ortho*-H_2^+ (*j odd*) are considered

v_r	v_b	v_s	$J=0$	$J=1^e$		$J=1^f$	$J=2^e$			$J=2^f$	
				$k=0$	$k=1$	$k=1$	$k=0$	$k=1$	$k=2$	$k=1$	$k=2$
0	0	0	(−2108.45)	5.14	636.99	637.07	15.42	647.28	1275.35	647.54	1275.35
0	0	1	810.72	4.89	577.18	577.30	14.66	586.85	1146.96	587.19	1146.96
0	2	0	1289.49	5.14	534.71	534.87	15.42	544.88	1059.28	545.34	1059.22
0	0	2	1513.64	4.60	512.88	513.06	13.79	521.73		522.26	
1	0	0	1747.24	5.07	550.13	549.87	15.20	560.93		560.21	
0	2	1	1864.53	4.74	523.35	523.44	14.21				
0	4	1	2107.99	4.31	397.03	396.41	12.93				
0	0	3	2156.27	4.76	396.93	397.23	14.29				

Table 7. Lowest $J = 1$ rotational levels in cm^{-1} relative to the lowest $J = 0$ vibrational level of the isotopomers of NeH_2^+. Explanations see Table 6

	$J = 1^e$		$J = 1^f$
	$k = 0$	$k = 1$	$k = 1$
		Fit 1	
NeH_2^+	5.25	650.35	651.44
$NeDH^+$	4.52	522.74	522.82
$NeHD^+$	3.08	614.01	614.04
NeD_2^+	2.86	473.84	473.87
		Fit 2	
NeH_2^+	5.22	673.50	673.58
$NeDH^+$	4.50	542.56	542.64
$NeHD^+$	3.06	636.64	636.67
NeD_2^+	2.84	492.51	492.28
		Fit 3	
NeH_2^+	5.14	637.00	637.08
$NeDH^+$	4.42	510.14	510.21
$NeHD^+$	3.02	601.58	601.61
NeD_2^+	2.80	462.25	462.28

The difference in the three surfaces is $\approx 40\ cm^{-1}$ for the zero-point energy, where Fit 3 leads to lower fundamental frequencies. The Ne–H_2^+ stretching frequency is (849.5, 858.6, 810.7 cm^{-1} for Fit 1, 2, 3, resp.) and the next higher mode is the Ne–H–H^+ bending (1198.0, 1228.4, 1198.4 cm^{-1}). The first excited H_2^+ vibration is strongly mixed with the Ne–H_2^+ stretching mode (see 9th and 10th state in Figs. 1 and 4a). In comparison with the fundamental frequency of free H_2^+ ($\omega = 2187.4$, 2187.4, 2169.4 cm^{-1}), the complex formation with Ne has reduced the fundamental frequency by $\approx 500\ cm^{-1}$ (more than 20%).

Although the barrier for H_2^+ rotation at $\theta = 90°$ is ≈ 957–$1190\ cm^{-1}$ for the three different fits (see Table 1) above ZPE, the states 11 and 12 at $E = 1884\ cm^{-1}$ above ZPE (see Fig. 2) show a splitting or destruction of degeneracy of only $0.9\ cm^{-1}$ (Fit 3; and nearly $4\ cm^{-1}$ in Fits 1, 2) (Table 5). In the case of NeD_2^+ (Table 4) the fundamental R-stretching and θ-bending modes are reduced to (656.9, 662.9, 622.5 cm^{-1}) and (902.8, 930.1, 888.7 cm^{-1}). The first excited D_2^+ vibration lies at 1486.7 cm^{-1} (Fit 1). The breaking of degeneracy becomes first visible at 2340 cm^{-1} (Fit 1), some higher states are still degenerate.

In the case of asymmetric mass combinations, the collinear $NeDH^+$ is more stable than $NeHD^+$. The values for the ZPE and special vibrational frequencies are between the ones for NeH_2^+ and NeD_2^+ (compare Tables 2, 3, 4 and Figs. 2–4).

The interpretation of the wavefunctions shows that the molecule remains relatively compact in each potential minimum, but in each minimum the strong normal mode coupling does not allow a clear cut classification with respect to the corresponding quantum numbers. For bound states which lie above 2000 cm^{-1}

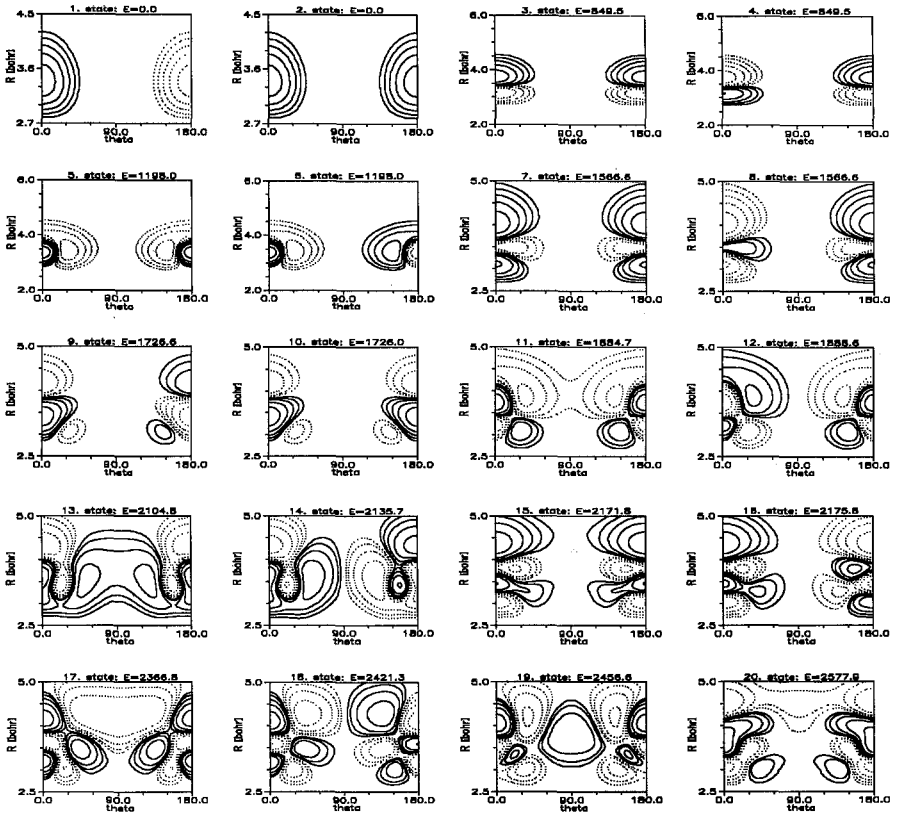

Fig. 2. [NeH_2^+]: Wavefunctions of the first 20 rovibrational states [Fit 1] for $J = 0$ with j even (for graphs 2, 3, 5, . .) and j odd (for graphs 1, 4, 6, . .). The plots are for H_2^+ frozen at $r = 2.0$ a_0. Contours are given for 64%, 32%, 16%, 8%, 4% of the maximum amplitude of the wavefunction. Solid (*dotted*) curves represent positive (negative) values of the amplitude. R is the distance between Ne and the center of mass of H_2^+, θ is the angle between R and the diatomic bond r of H_2^+. Energies are given in cm^{-1} and R is given in a_0

(in case of NeH_2^+), the wavefunctions are very diffuse and the calculated energies are rather different for the three surfaces, i.e. not very significant.

The calculated rovibrational states of NeH_2^+ for $J = 0, 1, 2$ are shown in Table 6. NeH_2^+ has linear geometry at the potential minimum and from inspection of Table 6 it can be interpreted as nearly rigidly linear. The quantum number k (k is a good quantum number for rigid molecules without coriolis coupling) is a rather good quantum number for the lowest states corresponding to the small splitting for e and f parity states. This splitting is lifted a little bit by bending.

The lowest rotational states for $J = 1$ are compared in Table 7. It shows that for low lying levels the rovibrational states are nearly degenerate and that there is very little tunneling in a complex with Ne always at the end of the complex. The differences between the three surfaces results in frequency-differences of $< 0.2\ cm^{-1}$ for $J = 1$, $k = 0$ and of $\approx 40\ cm^{-1}$ for $J = 1$, $k = 1$. The rotational constants B for NeH_2^+ are given as $2B = (5.25, 5.22, 5.14\ cm^{-1})$, the values for NeD_2^+ are a factor of 2 smaller.

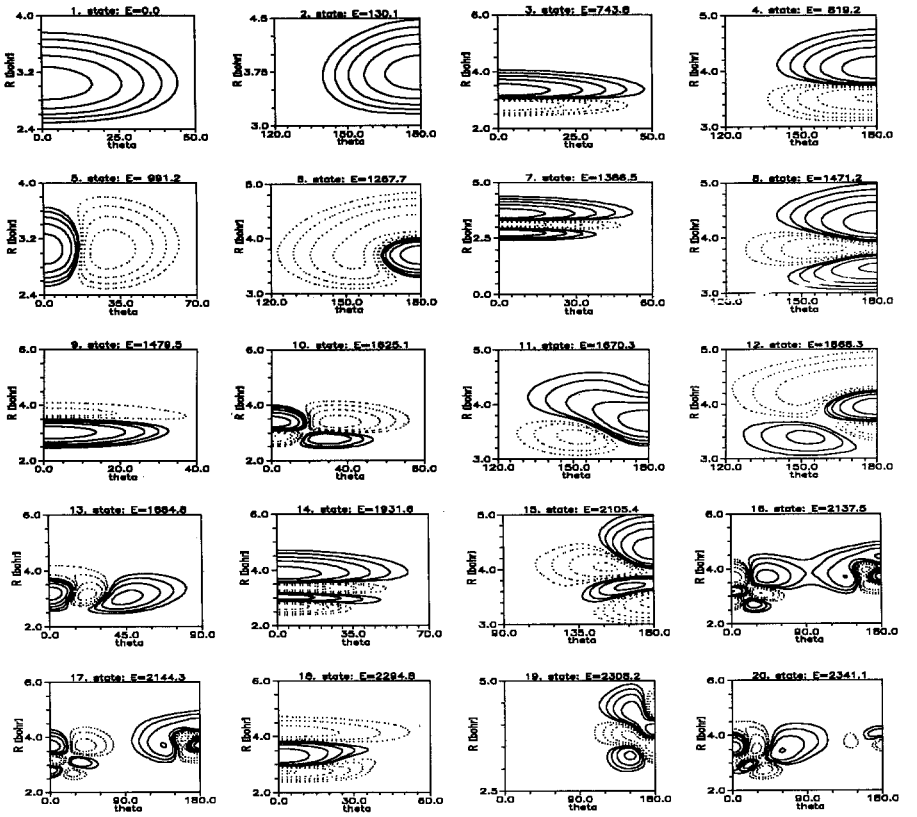

Fig. 3. Same as Fig. 2, but for [$NeDH^+$, $NeHD^+$]

The differences in the results for the three different surfaces are caused by the use of potential functions which are more concerned with fitting all the features required for reaction dynamics than with getting a highly accurate representation of the spectroscopically important region about the potential minimum. In a further work we will try to get a better fit around the potential minimum, but nevertheless the now used global surfaces give a clear impression of the rovibrational states.

How many bound states do exist for NeH_2^+? We will discuss this question for example for Fit 3 ($J = 0$), using 1200 product functions where the convergence is good up to the dissociation limit. The given total numbers of bound states are lower bounds to the exact numbers. The electronic energy minimum lies at collinear Ne–H–H^+ at $E_{\min,180°} = -4134\,\mathrm{cm}^{-1}$, the barrier lies at 90° at $E_{\min,90°} = -957\,\mathrm{cm}^{-1}$. The zero point energy is $-2108\,\mathrm{cm}^{-1}$ that is $\approx 3000\,\mathrm{cm}^{-1}$ below the asymptotic ZPE of the separated $Ne + H_2^+$ at $E_{Ne+H_2^+,ZPE} = +1084.7\,\mathrm{cm}^{-1}$. Only the ground state at $E = -2108\,\mathrm{cm}^{-1}$ and the first excited state at $E = -1298\,\mathrm{cm}^{-1}$ are below $E_{\min,90°}$ and 2*16 states (even and odd) in total are below the asymptotic ZPE (dissociation limit). For $J = 1$ there are 82 bound states (57 with *e*-parity, 25 with *f*-parity) and for $J = 2$ there are 118 bound states (75 with *e*-parity and 43 with *f*-parity).

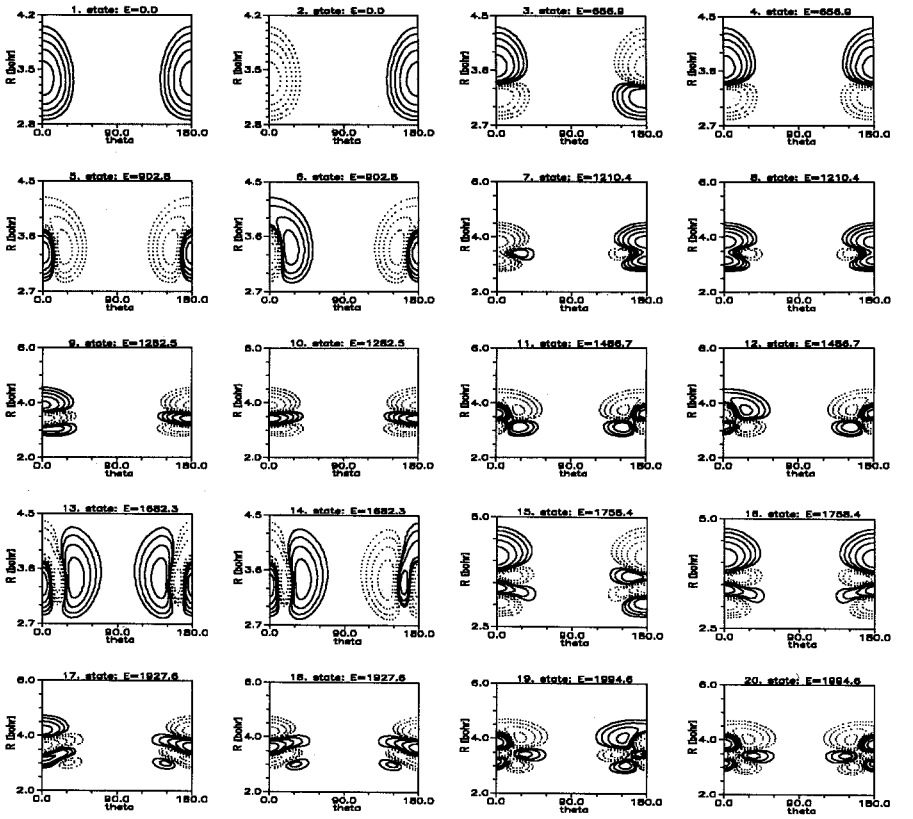

Fig. 4. Same as Fig. 2, but for $[NeD_2^+]$

4 Conclusions

Bound rotation-vibration levels of the NeH_2^+ complex have been predicted using three different fits of recently proposed potential energy surfaces [12]. We hope that the predicted levels will be useful for spectroscopists searching for the yet unobserved spectrum of this species. The root-mean-square error of the three fits to the *ab initio* surface is up to 242 cm^{-1}, which is the major source of error in our calculations. NeH_2^+ and its isotopomers can be approximated as linear molecules. For energies of $\approx 1900\ cm^{-1}$ above ZPE tunneling between the two states in the double minimum potential cannot be neglected. Although the barrier at 90° lies energetically near the first excited rovibrational state, the first five states of each symmetry (even or odd) show degeneracy within 1 cm^{-1}.

Fig. 5. Wavefunctions of H_2^+, HD^+, D_2^+ stretching modes [Fit 1] ($J = 0$, j even). The plots are for $\theta = 0°$ (**a**, **b**) and 180° (**c**, **d**, **e**). Contours are given for 64%, 32%, 16%, 8%, 4% of the maximum amplitude of the wavefunction. Solid (*broken*) curves represent positive (negative) values of the amplitude. R is the distance between Ne and the center of mass of H_2^+, r is the H_2^+ bond distance. Energies are given in cm^{-1} and lengths are given in a_0

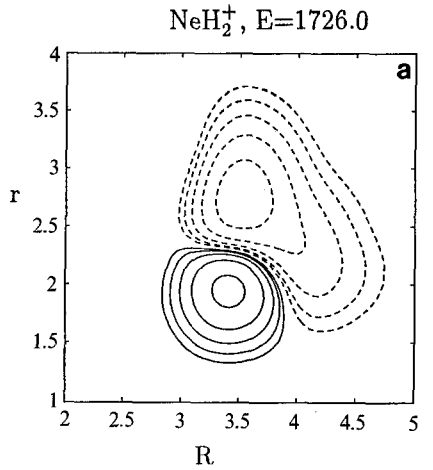
NeH$_2^+$, E=1726.0
a
r
R

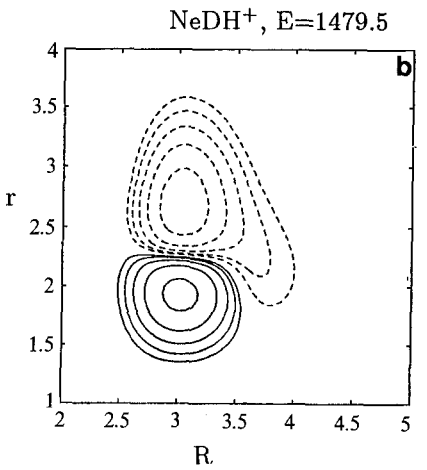
NeDH$^+$, E=1479.5
b
r
R

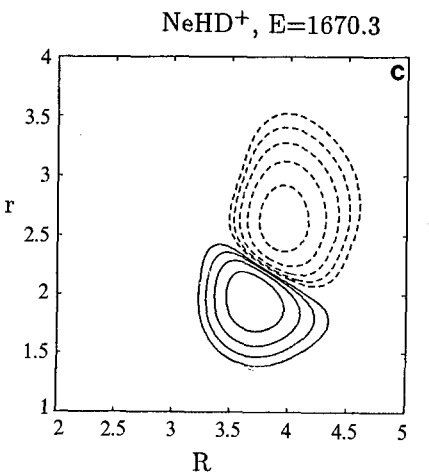
NeHD$^+$, E=1670.3
c
r
R

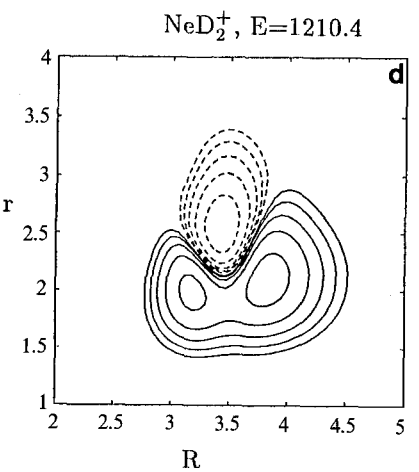
NeD$_2^+$, E=1210.4
d
r
R

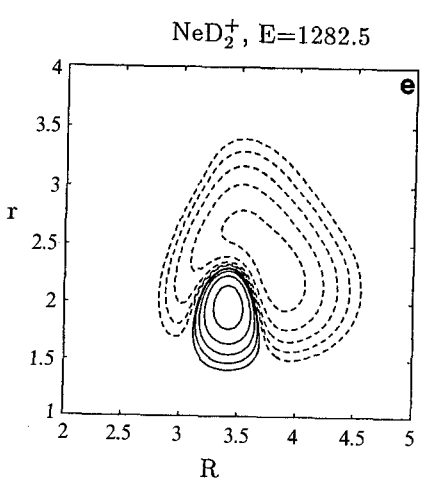
NeD$_2^+$, E=1282.5
e
r
R

NeH_2^+ is similar to HeH_2^+ system, which has also linear geometry but only half the binding energy. In contrast to NeH_2^+, one does not find an excited H_2^+ stretching mode in HeH_2^+.

In a further work we will try to characterize the quasibound states where a comparison with scattering resonances would be most interesting [11]. The quasibound states we calculated so far are too different for the three different fits in order to make any suggestions with respect to resonances. A further improvement of the fits seem to be necessary.

Acknowledgements. The author thanks Dr. J. Tennyson for help in using the TRIATOM program package and Prof. V. Staemmler and Prof. W. H. E. Schwarz for helpful comments. Computer time on the Cray-YMP in Jülich (Germany) is greatfully acknowledged.

References

1. Maier JP (1988) Ion and cluster ion spectroscopy and structure. Elsevier, Amsterdam
2a. Chupka WA, Russell ME (1968) J Chem Phys 49:5426
2b. Bilotta RM, Farrar JM (1981) J Chem Phys 75:1776
2c. van Pijkeren D, van Eck J, Niehaus A (1983) Chem Phys Lett 96:20
2d. van Pijkeren D, Boltjes E, van Eck J, Niehaus A (1984) Chem Phys 91:293
2e. Herman Z, Koyano I (1987) J Chem Soc, Faraday Trans II 83:127
2f. Ervin KM, Armentrout PB (1987) J Chem Phys 86:6240
2g. Gerlich D, Schweizer M (1989) Europhysics Conf Abstracts, Vol 13C, part 1, p 100
3. Kuntz PJ, Roach AC (1972) J Chem Soc, Faraday Trans II 68:259
4. Vasudevan K (1975) Mol Phys 30:437
5. Bolotin AB, Bugaets OP, Zhogolev DA (1976) Chem Phys Lett 37:9
6. Hayes EF, Siu AKQ, Chapman FM Jr., Matcha RL (1976) J Chem Phys 65:1901
7. Stroud C, Raff LM (1980) Chem Phys 46:313
8. Zuhrt C (1989) in: Popielawski J (ed) Proc Int Symp, The Dynamics of Systems with Chemical Reactions. Swidno Poland, June 6–10, 1988. World Scientific, Singapore, 253
9. Urban J, Jaquet R, Staemmler V (1990) Int J Quantum Chem 38:339
10. Urban J, Klimo V, Staemmler V, Jaquet R (1991) Z Phys D 21:329
11. Kress JD (1991) Chem Phys Lett 179:510
12. Pendergast P, Heck JM, Hayes EF, Jaquet R (1993) J Chem Phys 98:4543
13. Tennyson J, Miller S (1987) J Chem Phys 87:6648
14. Staemmler V, Jaquet R (1981) Theoret Chim Acta 59:487
15. Joseph T, Sathyamurthy N (1987) J Chem Phys 86:704
16. Sorbie KS, Murrell JN (1975) Mol Phys 29:1387
17. Schinke R (1984) J Chem Phys 80:5510
18. Aguado A, Paniagua M (1992) J Chem Phys 96:1265
19. Ischtwan J, Smith BJ, Collins MA, Radom L (1992) J Chem Phys 97:1191
20. Sutcliffe BT, Tennyson J (1991) Int J Quant Chem 29:183
21. Tennyson J, Miller S (1989) Comp Phys Comm 55:149
22. Miller S, Tennyson J (1987) J Mol Spectrosc 128:183
23. Jaquet R, Padkjaer S, to be published
24. Brown JM, Hougen JT, Huber KP, Johns JWC, Kopp I, Lefrebvre-Brion H, Merer AJ, Ramsay DA, Rostos J, Zare RN (1975) J Mol Spectrosc 55:500